Cooperative Atomic Displacements and Melting at the Limit of Superheating

Francesco Delogu*

Dipartimento di Ingegneria Chimica e Materiali, Università degli Studi di Cagliari, piazza d'Armi, I-09123 Cagliari, Italy

Received: August 8, 2005; In Final Form: December 23, 2005

This paper shows how the melting of superheated crystals originates from the localization of thermal disorder in excited regions of the crystalline structure. Within such regions, disordered thermal motion is found to induce the formation of bulk topological defects. These consist of atoms with a number of nearest neighbors different from the equilibrium one. Such defectively coordinated atoms arrange according to pseudolinear clusters, the number and size of which depend on temperature. Characterized by high mobility, defective atoms and their nearest neighbors are seen to undergo a cooperative dynamics that can result in net atom displacements between equilibrium lattice sites.

I. Introduction

Whenever melting at surfaces, interfaces, and structural defects is suppressed, crystalline structures can attain considerable degrees of superheating.[1−4] The region of metastability above the thermodynamic melting point T_m that a solid can explore is predicted to have boundaries of thermodynamic and kinetic nature.[5−8] The ultimate limit to superheating is identified by the so-called Born criterion for melting, which predicts the occurrence of a "rigidity catastrophe" at temperatures on the order of 1.6 T_m.[7,8] The first limit to superheating, arising at temperatures of about 1.16 T_m, is connected instead with the homogeneous nucleation of the molten phase in the ideal, defect-free crystal bulk and is essentially kinetic.[9] It is not, however, completely unrelated to the Born criterion. It has been shown indeed that vibrational disorder self-organizes in clusters of atoms highly displaced from equilibrium positions. Within such clusters, the shear modulus vanishes, so inducing the local mechanical failure of the crystalline lattice.[9] Not only does this demonstrate the existence of an unexpected connection between the Lindemann and Born criteria on the atomic scale,[10] but it also suggests that such criteria could both be rationalized within the framework of defect-mediated melting theories.[11−16] The formation of clusters of atoms satisfying a Lindemann criterion implies indeed the localization of vibrational disorder in particular regions of solid, and it is exactly in those regions that topological defects are expected to form more likely. The present work studies the properties of such topological defects and their role in the mechanism of melting at the limit of superheating. In particular, it is focused on the atomic scale processes governing the dynamics of atoms belonging to defective structures. Numerical simulations were employed to gain the necessary insight into the mechanisms of generation and evolution of such atoms. In the following, the numerical procedures adopted are described in detail.

II. Numerical Simulations

Molecular dynamics (MD) simulations were used to explore the atomic scale dynamics of a system of 6912 atoms arranged on a cF4 face-centered-cubic (fcc) lattice, the simulation box having 12 elementary crystallographic cells along each Cartesian direction. Periodic boundary conditions were applied along the three Cartesian directions to simulate a perfect bulk.[17] Interactions between the N atoms were described by a Lennard-Jones (LJ) pair potential:[17]

$$V_{LJ}(r) = 4\epsilon\left[\left(\frac{\sigma}{r}\right)^{12} - \left(\frac{\sigma}{r}\right)^{6}\right] \quad (1)$$

The LJ parameters for Ar atoms were employed, that is, a LJ diameter $\sigma = 3.405$ Å and an energy well depth $\epsilon = 1.65 \times 10^{-21}$ J. The nearest-neighbors' equilibrium distance at 0 K, $r_0 = 2^{1/6}\sigma$, defined the initial crystallographic cell constant $a_0 = 2^{1/2}r_0$. Forces were computed for distances r extending to a spherical cutoff radius $r_c = 3\sigma$ approximately corresponding to the ninth shell of nearest neighbors. Nosè-Hoover and Andersen thermostats were applied to sample the *NPT* ensemble dynamics at constant number of atoms N, pressure P, and temperature T.[18,19] The Parrinello−Rahman scheme was implemented for allowing the system to eventually undergo phase transformations requiring a change of the shape of the elementary crystallographic cell.[20] A fifth-order predictor-corrector algorithm and a time step $\delta t = 5$ fs were employed to solve the equations of motion. The system was initially equilibrated for 2×10^4 time steps at an external pressure $P \approx 0$ and a temperature $T = 60$ K. It was then slowly heated by imposing temperature jumps $\Delta T = 0.05$ K in a single time step and successive equilibration stages of 2500 time steps. The decrease of long-range crystalline order was monitored by means of the static order parameter:[17]

$$S(\boldsymbol{k}) = \frac{1}{N}\{[\sum_{i=1}^{N}\cos(\boldsymbol{k}\cdot\boldsymbol{r}_i)]^2 + [\sum_{i=1}^{N}\sin(\boldsymbol{k}\cdot\boldsymbol{r}_i)]^2\}^{1/2} \quad (2)$$

where the wave vector $\boldsymbol{k}$ is a reciprocal lattice vector and the vector $\boldsymbol{r}_i$ defines the position of the ith atom. $S(\boldsymbol{k})$, which equals unity for an ideal crystal at 0 K and approaches zero in the liquid,[17] was evaluated with reference to the [100] and [111] $\boldsymbol{k}$ vectors.

As successively discussed in detail, the gradual increase of temperature determines the appearance of topological defects in the initially defect-free crystal bulk. The processes governing the generation and evolution of such defects can be properly

* Corresponding author. E-mail: delogu@dicm.unica.it.

10.1021/jp0544078 CCC: $33.50
Published on Web 02/03/2006

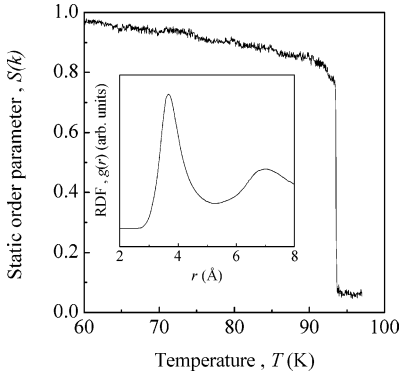

Figure 1. The static order parameter, $S(\boldsymbol{k})$, as a function of temperature T. Homogeneous melting is marked by the sudden drop in $S(\boldsymbol{k})$ values at T_m^K and determines the formation of an isotropic liquid phase, as shown by the RDF $g(r)$ quoted in the inset.

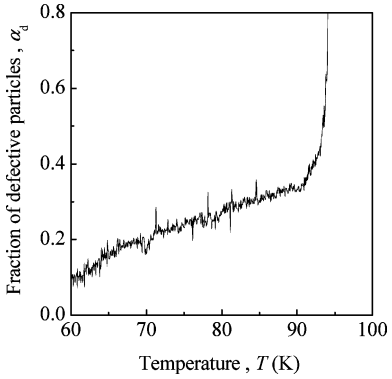

Figure 2. The fraction of defective atoms, α_d, as a function of temperature T. Homogeneous melting takes place when α_d amounts to about 0.4.

studied by looking at those atoms, hereafter referred to as defective atoms, characterized by a defective coordination.[16] More specifically, a defective atom is here defined as an atom with a number of nearest neighbors different from 12, the characteristic coordination number for fcc lattices. A distance criterion is employed to evaluate the number of nearest neighbors. Accordingly, two atoms are considered as nearest neighbors when their distance is lower than the distance r_{min} corresponding to the first minimum in the radial distribution function (RDF) $g(r)$ of the fcc solid. In addition, the so-called Honeycutt−Andersen parameters[21] were employed to monitor the local structural order in crystalline regions and eventually identify arrangements of atomic species according to regular lattices different from the fcc one, in particular the hexagonal-close-packed (hcp) ordering. This permits one to point out the possible formation of stacking faults, which have to be regarded as defective regions even though the number of coordinated neighbors around each atom involved remains 12.

III. Results and Discussion

The static order parameter $S(\boldsymbol{k})$ undergoes a gradual decrease as the temperature T increases, pointing out a contemporary decrease of the long-range crystalline order. The gradual $S(\boldsymbol{k})$ decrease is followed by a sudden drop, as evident from the plot of $S(\boldsymbol{k})$ values quoted in Figure 1 as a function of temperature T. The drop unambiguously identifies the homogeneous melting of the crystalline bulk at a temperature $T_m^K = 93.5$ K, that is, approximately 13 K above the equilibrium melting point T_m for the potential employed.[22] As proven by the RDF reported in the inset in Figure 1, the homogeneous melting results in the formation of an isotropic liquid phase.

III. 1. Characterization of Structural Disorder. The gradual $S(\boldsymbol{k})$ decrease preceding the sudden drop and then the homogeneous melting is caused by the increase of structural disorder due to the increase of the average amplitude of atomic vibrations. These, in turn, induce the formation of an increasing number of structural defects. The formation of such defects is marked by the appearance of atoms with a number of nearest neighbors different from 12, the equilibrium coordination number in fcc lattices. The formation of defective atoms requires then a change in the nearest neighbors' coordination shells of two neighboring atoms A and B. The mechanism underlying the formation of defective atom pairs requires in particular that when A loses one of its nearest neighbors, the distance of which has become larger than r_{min}, B accepts it in the coordination shell. Accordingly, A assumes a coordination number equal to 11, while B assumes a coordination number equal to 13. As shown in Figure 2, the fraction α_d of defective atoms, defined as the ratio between the number of defective atoms and the total number of atoms in the system, increases as the temperature T increases. In satisfactory agreement with previous observations of Gomez et al.,[16] melting occurs when α_d amounts approximately to 0.4.

Because of the generation of atoms with defective coordination, two different atom subsets can be identified within the simulated system. The first subset is the larger one and consists of those atoms retaining the normal 12-fold coordination. The second one includes, instead, those atoms with a number of nearest neighbors different from 12. In this sense, the system can be then regarded as heterogeneous. A further reason to regard the system as heterogeneous is provided by the analysis of local crystalline order by means of the Honeycutt−Andersen parameters.[21] It reveals indeed that stacking faults occasionally appear as a consequence of a temporary modification of the planar stacking due to a transition from the fcc to the hcp crystalline arrangement. The size of hcp domains, on the order of 2−3 nm and involving 15−20 atoms each, does not show a significant dependence on temperature T. Strongly dependent on temperature are instead the number and the average lifetimes of hcp domains. At relatively low temperatures, a small number of stacking faults, about 20, is observed, with an average lifetime of approximately 8 ns. At high temperatures, the number of hcp domains increases up to about 100. However, the average lifetime decreases to only 1−2 ns, so that hcp domains become very labile local structures continuously forming and disappearing in the fcc crystalline bulk structure.

III. 2. Dynamics of Defective Atoms. The hcp domains are bounded by atoms with defective coordination, which then display a certain degree of spatial organization. Their arrangement can be studied by monitoring the relative position of atoms showing spatial and dynamical correlation. The distance criterion employed to identify defective atoms has been further applied to evaluate the degree of their spatial correlation via the calculation of the number of defective atoms belonging to a given cluster and, in turn, the total number of clusters N_{cl}. According to the distance criterion employed, two defective atoms have been then regarded as belonging to the same cluster when their distance was shorter than r_{min}.

The analysis of defective atom positions reveals that at relatively low temperatures the generation of defective atom pairs takes place apparently randomly in the bulk and the generated defective atom pairs are relatively distant from the other ones already present in the system. As the temperature increases, however, defective atoms appear cooperatively in the same regions of solid and form extended pseudolinear clusters.

The number and size of clusters depend then on temperature.

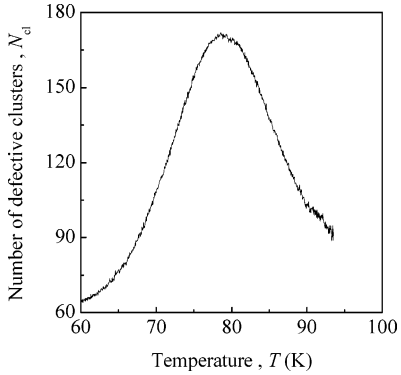

Figure 3. The number of defective atom clusters, N_{cl}, as a function of temperature T. N_{cl} attains a maximum at about 0.8 T_m^K and is successively limited by cluster coalescence processes.

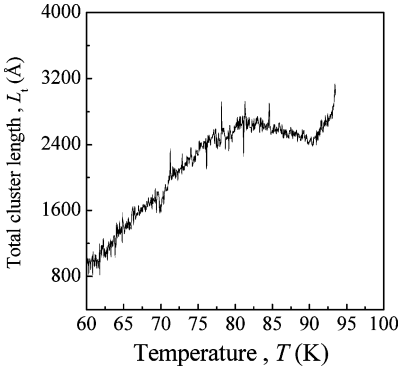

Figure 4. The total length of defective atom clusters, L_t, as a function of temperature T. The coalescence of different clusters limits the increase of L_t in the temperature range between 80 and 90 K. At higher temperatures, the growth of the number of defective atom prevails over other factors, determining a marked L_t increase.

It can be seen from Figure 3 that N_{cl} increases regularly up to a temperature $T \approx 0.8\ T_m^K$, while at higher temperatures it undergoes a definite decrease. This behavior can be ascribed to the occurrence of cluster coalescence processes that become more and more probable as the size of single clusters increases. Under such circumstances, even though the number of defective atoms continues to increase, the total number of clusters N_{cl} rapidly decreases. It is here worth noting that a similar behavior should also be expected if the size of defective atom clusters would approach the sample size. To investigate possible effects of the system size, simulations have been also performed on smaller systems containing 2048 and 4000 atoms. In all of the cases, calculations yielded results very similar to the ones pertaining to the system of 6912 atoms. Such results permit one to reasonably exclude that the system size could significantly affect the system evolution and, correspondingly, the behavior observed.

Additional simulations were also performed on the system of 6912 atoms to investigate the possible occurrence of hysteresis in the generation of defective atoms and in the change with temperature of the fraction α_d of defective atoms as well as the number N_{cl} of defective atom clusters. To this aim, the system of 6912 atoms was relaxed at 65, 70, 75, 80, and 85 K to independently simulate five different points in the thermodynamic phase diagram. In each case, after relaxation the system dynamics was followed for 5000 time steps, and both the average fraction α_d of defective atoms and the average number N_{cl} of defective atoms clusters were evaluated. The α_d and N_{cl} values so obtained agree within about 4% with the α_d and N_{cl} values worked out, at the corresponding temperatures, by the simulations carried out under conditions of gradual temperature increase.

With the aim of definitely excluding hysteresis effects, the atomic configurations relaxed at 70 and 85 K were further subjected to a gradual temperature decrease of 0.05 K every 2500 time steps to attain the temperatures of 65 and 80 K, respectively. At such temperatures, the α_d and N_{cl} average values were once more evaluated and compared to the ones previously obtained. A correspondence within 4−5% was observed. Such results permit one to exclude hysteresis effects.

The total spatial extension of clusters is related to the cluster size. A measure of the spatial extension of the clusters is given by the total length of clusters L_t, quoted in Figure 4 as a function of temperature T, defined as the sum of single cluster lengths L_j, L_j being the maximum distance between two atoms in the jth cluster.[16,23] Data in Figure 4 show that L_t undergoes a smooth increase in the temperature range between 60 and about 80 K. In the neighborhood of 80 K, that is, approximately in correspondence with the maximum in the N_{cl} curve, a gradual change in slope is observed. Within the temperature range between 80 and 90 K, the total cluster length L_t slightly decreases as a consequence of the decrease in the number N_{cl} of clusters. However, the increase in the number of defective atoms prevails on the N_{cl} decrease as the homogeneous melting point T_m^K is approached and determines the final steep L_t increase observed.

Defective atom clusters display a variegated topology, the analysis of which reveals that clusters can be occasionally regarded as lattice defects. At low temperatures, clusters consist of a small number of defective atoms. Under such circumstances, the geometrical properties of one such small cluster rarely correspond to the geometrical properties of either a dislocation line or a dislocation loop. As the temperature increases, however, even though the mobility of defective atoms and of their nearest neighbors also increases, the number of clusters possessing the characteristics of dislocations increases. It becomes then possible to identify Shockley partial dislocations as well as, although more rarely, dislocation lines crossing the whole system particularly in the vicinity of the homogeneous melting point T_m^K. Even in this temperature range, however, a certain number of defective atom clusters cannot be interpreted as true dislocations.

One of the reasons hindering the identification of lattice defects is represented by the high mobility of defective atoms and their nearest neighbors, which continuously rearrange their positions. Under such conditions, it is difficult to distinguish between a thermal vibration of large amplitude and an actual rearrangement of atomic positions. Because of the short time periods during which such processes occur, it is also difficult to define properly the average position of a given atom. As a consequence of such behavior on short, relatively temperature-dependent time scales, defective atom clusters appear as dynamical entities evolving in time, with atoms continuously joining and leaving a given cluster as a consequence of their local mobility. The continuous atom replacement processes modify the cluster size and configuration as well as its position. Defective atom clusters can then move and interact via ramification, fragmentation, and coalescence events. Such processes have rates governed by the time period τ over which a given atom belongs to a given cluster, also referred to as the lifetime of atom in cluster. This quantity is expected to depend on the average potential energy U the atom has within the cluster in the period τ.

III. 3. Dynamical Heterogeneities. It is here necessary to define the lifetime τ of defective atoms in clusters without

ambiguities and describe in detail how such quantity is evaluated. The precise definition of τ poses some difficulties. It is not rare, indeed, to observe atoms undergoing successive modifications in the number of nearest neighbors in a small number of time steps. This occurs particularly at high temperatures, when the disordered thermal motion of atoms undergoing large amplitude vibrations can determine rapid configurational changes in the nearest neighbors' shell. For example, it can happen that a 12-fold coordinated atom could maintain its normal coordination for relatively long times and become defective for only few tenths of time steps. It does not seem reasonable to consider such an atom as defective. In addition, taking into account every change in coordination without considering the time scales over which such changes take place would introduce large fluctuations in the quantities calculated. For this reason, the dynamics of defective atoms was accurately monitored to find a significant threshold value of τ below which the atom experiences a defective coordination for too short times to be considered as defective. Within this framework, defective atoms were seen to undergo a relatively simple dynamical behavior. At a temperature of 60 K, the largest fraction of defective atoms, up to about 95%, keeps the defective coordination for times on the order of 300 ps or longer. The remaining 5% of defective atoms is subjected to frequent changes in the nearest neighbors' shell configuration. However, these atoms do not keep the same defective configuration for times longer than 20 ps, corresponding to about 400 time steps. At temperatures close to T_m^K, such time is even shorter due to the increased thermal vibrations. According to this evidence, the threshold value for τ was chosen equal to 50 ps. Therefore, in this second part of the study specifically dealing with energies and lifetimes of defective atoms, an atom is considered as defective whenever its coordination remains defective for times longer than 50 ps. As mentioned before, this threshold value excludes only about the 5% of defective atoms.

III. 4. Local Rearrangements of Atomic Positions. To gain insight into the cluster dynamics and characterize the structural and energetic heterogeneity of the simulated system, potential energies and lifetimes of single atoms in clusters were evaluated at five different temperatures. Simulations were carried out in three stages.[24] A *NPT* run of 2×10^4 time steps was used to adjust pressure and temperature, bringing the system to the desired thermodynamic state point. The system was then relaxed in *NVT*, that is, at constant number of atoms *N*, volume *V*, and temperature *T*, for additional 2×10^4 time steps to test possible undesired drifts in pressure or potential energy *U*. In the absence of drifts, the system was finally relaxed in *NVE*, that is, at constant number of atoms *N*, volume *V*, and energy *E*, to avoid the coupling with heat and pressure baths and their effects on dynamics.[17−19] The dynamics was then analyzed for 5×10^6 time steps. The distributions $f(U)$ of potential energy for defective and normally coordinated atoms as well as the lifetimes τ of defective atoms as a function of their potential energy *U* were evaluated by averaging over the whole time interval of 5×10^5 time steps. In particular, given a defective atom, its potential energy *U* during the time interval τ was recorded step by step. At the end of the time interval τ, that is, when the atom returns to a normal coordination, the potential energy values recorded were averaged to obtain a representative mean value. This latter value was then correlated to the lifetime τ.

Distributions obtained at $T \approx 0.75\ T_m^K$ are shown in Figure 5. They have a Gaussian-like shape and differ by a small relative shift of the mean value, defective atoms possessing on the average a higher potential energy. Distributions obtained at higher temperatures do not differ qualitatively from the ones shown. Because of the higher temperature, a curve shift toward higher energy values is only observed together with a slight broadening of Gaussian-like curves. The large superposition in energy distributions $f(U)$ indicates that the potential energy *U* is not the best parameter to consider for distinguishing the atom subsets and characterizing the system heterogeneity. Despite this, the potential energy is found to heavily affect the behavior of defective atoms and the cluster dynamics. The lifetime τ is indeed strongly dependent on *U*. It can be clearly seen from Figure 6, where ln τ is quoted as a function of *U*/*N*. A linear plot with negative slope is obtained, which indicates that atoms with high potential energy have a higher probability of leaving the cluster than atoms with low potential energy.

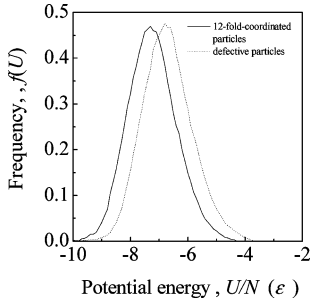

Figure 5. Potential energy distributions, $f(U)$, for normally coordinated (full line) and defective (dotted line) atoms. Areas under the curves are normalized to 1. Data refer to a temperature $T \approx 80$ K.

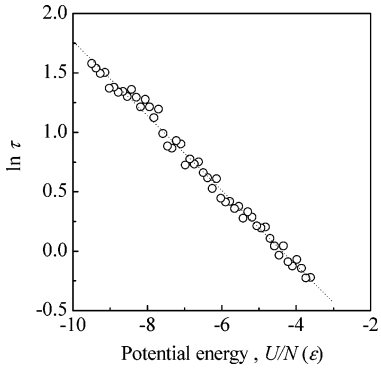

Figure 6. The logarithm of lifetime τ of atoms in clusters as a function of the potential energy per atom *U*/*N*. Data refer to a temperature $T \approx 80$ K. The best-fitted line is also shown.

The study of the atomic configurations of defective atoms permitted one to distinguish at least qualitatively between defective atoms with low and high potential energy. It appears that defective atoms having 3 or 4 defective atoms among nearest neighbors possess a low potential energy. This seems to be the consequence of the local relaxation of configurational strains due to the interaction and rearrangement of the nearest neighbors' shells of the different neighboring defective atoms. The defective atoms having 3 or 4 other defective atoms in the coordination shell are generally located in the core region of the defective atom cluster to which they belong. They lower their potential energy by a collective rearrangement of the positions of all of the defective atoms in the nearest neighbors' shell. In this way, local strains are easily relieved. Defective atom pairs embedded in a matrix of 12-fold coordinated atoms are instead subjected to higher local strains and then possess higher potential energy. A potential energy higher than the average is also characteristic of both defective atoms in small clusters and defective atoms in the final part of a string-like cluster. Such atoms have only 1 or 2 defective atoms in the coordination shell, and the accommodation of local strains is

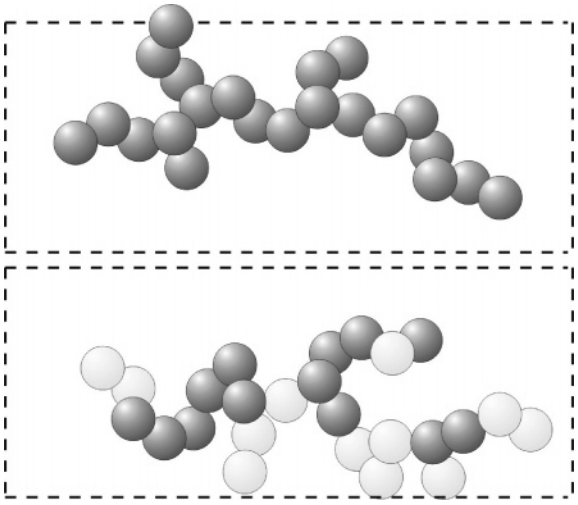

Figure 7. Planar projections of two configurations of a given cluster at $T \approx 80$ K at times 1 ns distant. Dark gray marks the atoms belonging to the cluster at the beginning of the 1 ns time interval (upper panel). Light gray marks those atoms that belong to the cluster at the end of time interval but did not belong to it at the beginning (lower panel). In the final configuration (lower panel), both dark and light gray atoms are present, indicating that not all of the atoms in the initial cluster configuration have been replaced. Dashed lines mark the region of solid considered and can be used as a reference framework to evaluate the configurational and positional change of the cluster.

more difficult, requiring the rearrangement of atom positions along a pseudolinear aggregate of defective atoms surrounded by atoms with normal coordination. Under such circumstances, a change in the number of nearest neighbors is much more effective in relaxing the local configuration of these atoms than the rearrangement of positions along the linear cluster. Defective atoms suffering high local strain can then undergo a modification of the coordination shell with a probability higher than other defective atoms. Accordingly, low and high potential energies pertain, respectively, to highly relaxed or highly strained defective atom configurations.

Whenever a defective atom leaves the cluster, it restores its normal coordination, whereas one of its neighboring atoms becomes defective. The rearrangement of coordination shells requires a cooperative dynamics involving at least atoms with common nearest neighbors. More specifically, a series of contemporary atomic displacements take place, resulting in a net displacement of the defective atom cluster. To illustrate such a situation, defective atoms belonging to a small cluster are shown in Figure 7 at two successive simulation times. It can be seen that not only the cluster has assumed a different position, but also the total number of atoms involved in the cluster has changed. The cluster in the upper panel contains indeed 22 defective atoms, while the number of defective atoms in the lower panel is equal to 25. Furthermore, nine defective atoms belonging to the first configuration reported in the upper panel of Figure 7 have been replaced by other defective atoms during the time interval of 1 ns.

It is not easy to characterize in detail the microscopic processes ruling the rearrangement of coordination shells. The direct visualization of the group of atoms surrounding the ones undergoing the coordination shell modification indicates, however, that approximately 10−15 atoms on the average are directly involved in the collective rearrangement process. Such estimate is further supported by the analysis of the potential energy U of each atom involved in the rearrangement process. It appears indeed that the potential energy U of the atoms involved in the modification of the coordination shells undergoes

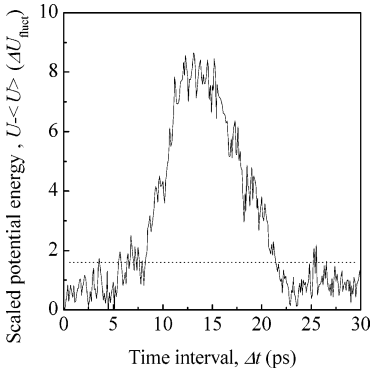

Figure 8. The rise of the potential energy U for the group of 14 atoms involved in the rearrangement of the coordination shells of two of them as a function of the time interval Δt. The potential energy U is scaled with respect to the average potential energy of the system, $\langle U \rangle$, and expressed in units of ΔU_{fluct} to point out the rise on a relative scale. The collective process of coordination shells rearrangement takes place on a time scale on the order of 10 ps. The rearrangement process took place at a temperature of about 0.7 T_m^K, that is, at about 65 K. The horizontal dotted line indicates the critical threshold U_c of potential energy equal to $1.6\Delta U_{fluct}$.

a definite shift toward higher values during the course of the rearrangement process. The rise in potential energy is more pronounced for the atoms nearest to the pair of atoms exchanging a nearest neighbor, that is, changing their coordination, and decreases gradually for more distant atoms. The decrease with distance is rapid, and eventual rises can be easily masked by normal potential energy fluctuations due to thermal vibrations. This evidence permits one to develop a relatively simple criterion for the rough identification of the atoms directly involved in the coordination shells rearrangement process based on the values of potential energy U they experience. More specifically, given a group of atoms surrounding a pair of atoms undergoing a modification of their coordination shells, the criterion establishes that the atoms involved in the rearrangement process are the ones in which the potential energy overcomes a critical threshold value U_c. In the present work, which discusses only a preliminary analysis of coordination shells rearrangement processes, the threshold value U_c was chosen so that the results of the analysis by direct visualization and by potential energy screening could approximately coincide. Such approximate coincidence was attained with a U_c value equal to 1.6 ΔU_{fluct}, where ΔU_{fluct} represents the average amplitude of potential energy fluctuations due to thermal vibrations. Although the procedure can seem rather arbitrary, it permits one to roughly estimate the number of atoms involved in a rearrangement process on the basis of a simple potential energy criterion. Unfortunately, relatively accurate estimates can be obtained only at low temperatures, that is, when the amplitude of thermal vibrations is not large. At such temperatures, the rise in potential energy U of the group of 10−15 atoms is evident. It can be seen in particular that their average potential energy U shows a maximum. An example of the potential energy U fluctuations undergone by a group of 14 atoms, 8 defectively coordinated and 6 normally coordinated, at about 0.6 T_m^K is given in Figure 8. The rise in potential energy ΔU observed is associated with the process leading to the modification of coordination shells. In this case in particular, one of the 12-fold coordinated atoms assumes a 11-fold coordination and one of its nearest neighbors changes its coordination from 11-fold to 12-fold. The rearrangement of nearest neighbors' shells takes place in a time interval of about 10 ps. The change of the coordination number of the two atoms involved is contemporary. During the transition

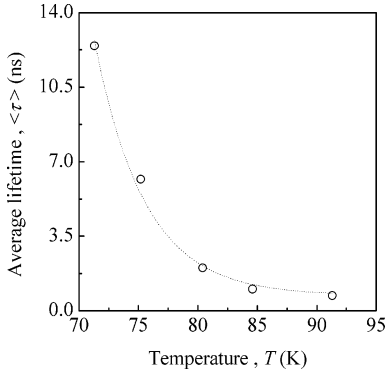

Figure 9. The average lifetime $\langle\tau\rangle$ of atoms in clusters as a function of the temperature T. An exponential trend is observed. The best fitted curve is also shown.

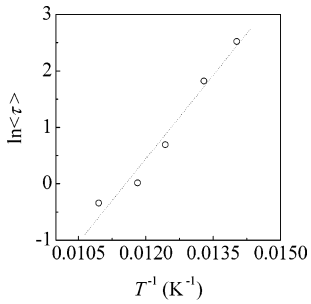

Figure 10. The logarithm of the average lifetime of atoms in clusters, $\ln\langle\tau\rangle$, as a function of the inverse of temperature, T^{-1}. The best fitted line is also shown.

stage, when one of the atoms is losing one of its nearest neighbors, which is going to be accepted in the coordination shell of the other atom involved, the group of 14 atoms is subjected to an increase of the local strain. This is signaled by the increase of the local potential energy U, that is, by the increase of the potential energy of the atoms belonging to the group. As the exchange of the nearest neighbor between the two atoms undergoing a modification of the coordination numbers has occurred, the local potential energy decreases and the atomic strain is relieved. Unfortunately, a systematic analysis of the exchange of nearest neighbors between neighboring atoms is extremely difficult, so that it is not possible to discuss here statistical results on a certain number of events of coordination shell modification. Even the partial evidence provided by the present preliminary analysis indicates, however, that the rearrangement process of coordination shells is a highly cooperative event.

III. 5. Self-Diffusion Processes. It is here worth noting that a given defective atom does not necessarily recover its original lattice position when it leaves the cluster of defective atoms by restoring its normal coordination. On the contrary, it often occupies a different lattice position. Therefore, the dynamics of defective atom clusters provides a mechanism for the self-diffusion of atoms on the lattice sites. The rate of self-diffusion processes mediated by the dynamics of defective atoms critically depends on the defective atom average lifetime $\langle\tau\rangle$. In particular, shorter lifetimes correspond to higher self-diffusion rates. As pointed out by data quoted in Figure 9, the average lifetime $\langle\tau\rangle$ of atoms in clusters decreases as the temperature increases. Thus, the mobility of defective atoms increases with temperature. The dependence of $\langle\tau\rangle$ on the temperature is significant. As demonstrated by the semilogarithmic plot shown in Figure 10, where a linear trend is obtained by quoting $\ln\langle\tau\rangle$ as a function of the inverse of temperature T^{-1}, the average lifetime $\langle\tau\rangle$ is an exponential function of temperature. It appears then that at any given temperature defective atoms have a mobility greater than the one of 12-fold-coordinated atoms. It is worth noting, however, that an enhanced mobility is also characteristic of the atoms that are nearest neighbors of defective ones. Whenever a defective atom leaves the cluster restoring its normal coordination, a neighboring atom becomes indeed defective. On the average, then, not only defective atoms in clusters but also their 12-fold coordinated neighbors possess a greater mobility than other atoms not directly involved in the cluster dynamics.

Evidence of defect-mediated self-diffusion processes in solid phases had already been discussed in a previous work.[25] It was shown that processes of atomic exchange on lattice sites take place as a consequence of the formation of vacancies and interstitials.[25] The present work supports such results and suggests that the average lifetime $\langle\tau\rangle$ concurs to determine the rate of self-diffusion processes. An apparent activation energy $E_a \approx 8.3$ kJ mol^{-1} can be obtained from the linear semilogarithmic plot in Figure 10 for the self-diffusion mechanism of atoms on lattice sites mediated by defective atoms. It is here worth noting that such apparent activation energy is related to the collective process of nearest neighbor shells' rearrangements mentioned above. It is then connected with the maximum of local potential energy of the small group of atoms rearranging their positions and coordination shells. Unfortunately, as discussed above, a detailed characterization of the dynamic processes associated with the rearrangement of coordination shells is not possible. Particularly at high temperatures, such characterization is hindered by thermal vibrations. A preliminary analysis on a restricted number of atomic configurations at a temperature of about 0.6 T_m^K seems to suggest that the rearrangement could be triggered by a thermally activated redistribution of volume among the atoms involved. It is, however, difficult to find a clear evidence of the correlation between volume, thermal energy localization, and coordination due to the relatively large fluctuations to which these quantities are subjected.

It is now interesting to note that the value of apparent activation energy E_a observed is considerably lower than the one of about 15.1 kJ mol^{-1} obtained from experimental investigation,[26] but not far from the activation energy of about 10.4 kJ mol^{-1} for self-diffusion in grain boundaries.[27] In addition, it is larger than the estimated activation energies for self-diffusion in surface layers, which amounts approximately to 5 kJ mol^{-1}.[28] The first E_a value mentioned above was obtained in diffusion experiments on an Ar crystal at low temperature,[26] while the other two were evaluated by means of numerical simulations on model Ar systems.[27,28] The comparison between the apparent activation energy E_a obtained in the present work and the ones reported above reveals that the diffusion process mediated by the dynamics of defective atoms takes place at rates that are roughly intermediate between those pertaining to diffusion processes in bulk and free surfaces. In particular, the closeness of the E_a value observed in the present work to the one for self-diffusion in grain boundaries[27] indicates that the diffusion process due to the continuous replacement of defective atoms in clusters and the diffusion process at grain boundaries occur with similar rates. This also suggests that the two diffusion processes could present common mechanistic features on the atomic scale. For example, atomic free volume, that is, the volume pertaining to single vibrating atoms that can be evaluated by applying the well-known Voronoi construction,[29,30] is expected to play an important role. It has been shown indeed that it is responsible for the lower activation energy E_a for diffusion observed in grain boundaries.[27] The evidence that

defective atoms in clusters have mobility and behavior apparently similar to the ones displayed by atoms at grain boundaries suggests that the free volume could also play an important role in the self-diffusion process mediated by defective atoms. A detailed study on the distribution of volume over the atoms and a comparison between the dynamics of atoms at grain boundaries and in defective atom clusters is currently under progress, and the results will be discussed in a future work.

It is finally worth noting that the experimental investigation of the self-diffusion process mediated by defective atom clusters is expected to present considerable difficulties. The most important one is related to the necessity of working with superheated crystals. The diffusion process becomes indeed observable only when a sufficient amount of defective atoms exists, and this occurs only at temperatures relatively close to the homogeneous melting point T_m^K. Unfortunately, superheating a crystalline phase presents considerable difficulties,[2−8] requiring, for example, the use of defect free single crystals to avoid the heterogeneous nucleation of the molten phase at lattice defects.[2−4] Under such circumstances, carrying out suitable experiments for investigating the diffusion process mediated by the dynamics of defective atoms is not an easy task. Another possibility of experimental investigation of the self-diffusion mechanism discussed in the present work could be the observation of anomalies in the diffusion process in normal crystals, for example, a self-diffusion faster than expected. However, it could be difficult in such case to distinguish between the effects of grain boundaries and those of defective atom clusters. The two processes are indeed expected to have similar activation energies.

IV. Summary and Conclusions

This work represents an attempt to characterize the dynamic processes responsible for the thermodynamic behavior of superheated crystals. Far from being exhaustive, the results obtained from the systematic investigation carried out define a conceptual framework based on the following observations of the present study: superheated crystals melt at a temperature T_m^K that is approximately 1.2 times the equilibrium melting point T_m for the interatomic potential used; because of the absence of free surfaces and interfaces, the melting process of superheated crystals relies upon the homogeneous nucleation of the molten phase in an initially, defect-free ideal bulk; thermally induced atomic vibrations generate, at relatively high temperatures, atoms with defective coordination; defective atoms undergo a cooperative dynamics, mediating the appearance of stacking faults and forming clusters, the size and number of which are temperature-dependent; the dynamics of defective atom clusters is governed by the average lifetime τ of atoms in clusters; the average lifetime τ of defective atoms in clusters is determined by the average potential energy U of defective atoms belonging to the clusters as well as of the normally coordinated atoms surrounding them; the rate of local rearrangements of atomic positions scales inversely with the average lifetime τ, and this, in turn, depends exponentially on the temperature; local rearrangements of atomic positions mediated by the dynamics of defective atoms result in the occurrence of an unusual self-diffusion of atomic species on the lattice sites; the average activation energy E_a of local rearrangements of atomic positions mediated by the dynamics of defective atoms displays a value close to the one of self-diffusion at grain boundaries and intermediate between the ones of self-diffusion at free surfaces and self-diffusion in the bulk due to point defects.

On the basis of the results mentioned above, it is possible to conclude that a superheated crystal is a dynamically heterogeneous system consisting of two subsets of atoms characterized by normal and defective coordination, respectively. As the temperature approaches the limit of superheating, that is, the homogeneous melting point, atoms with defective coordination appear cooperatively and form string-like clusters. Topological disorder is then localized in particular regions of solid and not homogeneously distributed in the bulk. Defective atoms have a greater mobility than normally coordinated atoms, and their continuous rearrangements not only modify the number, size, and configuration of clusters, but also provide a mechanism for self-diffusion. The comparison between the apparent activation energy for the self-diffusion process mediated by defective atoms and the ones pertaining to diffusion processes in the bulk, in grain boundaries, and in surface layers suggests that the self-diffusion process discussed in the present work presents similarities to the one in grain boundaries. Further work is needed to deepen the knowledge on this point.

Acknowledgment. Prof. G. Cocco, Dipartimento di Chimica, Università degli Studi di Sassari, and Dr. G. Manai, Department of Physics, Trinity College, Dublin, Ireland, are gratefully acknowledged for useful discussions. A. Ermini, ExtraInformatica s.r.l., is gratefully acknowledged for technical support. Financial support was provided by the University of Cagliari.

References and Notes

(1) Chandler, D. *Introduction to Modern Statistical Mechanics*; Oxford University Press: Oxford, 1987.

(2) Cormia, R. L.; Mackenzie, J. D.; Turnbull, D. *J. Appl. Phys.* **1963**, *34*, 2239.

(3) Cahn, R. W. *Nature* **1986**, *323*, 668.

(4) Maddox, J. *Nature* **1987**, *330*, 599.

(5) Lindemann, F. A. *Phys. Z.* **1910**, *11*, 609.

(6) Gilvarry, J. J. *Phys. Rev.* **1956**, *102*, 308.

(7) Born, M.; Huang, K. *Dynamical Theory of Crystal Lattices*; Clarendon Press: Oxford, 1954.

(8) Tallon, J. L. *Nature* **1989**, *342*, 658.

(9) Lu, K.; Li, Y. *Phys. Rev. Lett.* **1998**, *80*, 4474.

(10) Cahn, R. W. *Nature* **2001**, *413*, 582.

(11) Kosterlitz, J. M.; Thouless, D. J. *J. Phys. C* **1973**, *6*, 1181.

(12) Nelson, D. R.; Halperin, B. I. *Phys. Rev. B* **1979**, *19*, 2457.

(13) Young, P. *Phys. Rev. B* **1979**, *19*, 1855.

(14) Kleinert, H. *Gauge Theory in Condensed Matter*; World Scientific: Singapore, 1989.

(15) Burakovsky, L.; Preston, D. L.; Silbar, R. R. *Phys. Rev. B* **2000**, *61*, 15011.

(16) Gomez, L.; Dobry, A.; Geuting, C.; Diep, H. T.; Burakovsky, L. *Phys. Rev. Lett.* **2003**, *90*, 095701.

(17) Allen, M. P.; Tildesley, D. *Computer Simulation of Liquids*; Clarendon Press: Oxford, 1987.

(18) Nosè, S. *J. Chem. Phys.* **1984**, *81*, 511.

(19) Andersen, H. C. *J. Chem. Phys.* **1980**, *72*, 2384.

(20) Parrinello, M.; Rahman, A. *J. Appl. Phys.* **1981**, *52*, 7182.

(21) Honeycutt, J. D.; Andersen, H. C. *J. Phys. Chem.* **1987**, *91*, 4950.

(22) Broughton, J. Q.; Gilmer, G. H. *J. Chem. Phys.* **1983**, *79*, 5095.

(23) Braunstein, L. A.; Buldyrev, S. V.; Havlin, S.; Stanley, H. E. *Phys. Rev. E* **2002**, *65*, 056128.

(24) Donati, C.; Glotzer, S. C.; Poole, P. H.; Kob, W.; Plimpton, S. J. *Phys. Rev. E* **1999**, *60*, 3107.

(25) Lee, G. C. S.; Li, J. C. M. *Phys. Rev. B* **1989**, *39*, 9302.

(26) Parker, E. H. C.; Glyde, H. R.; Smith, B. L. *Phys. Rev.* **1968**, *176*, 1107.

(27) Ciccotti, G.; Guillope, M.; Pontikis, V. *Phys. Rev. B* **1983**, *27*, 5576.

(28) Rosato, V.; Ciccotti, G.; Pontikis, V. *Phys. Rev. B* **1986**, *33*, 1860.

(29) Tanemura, M.; Ogawa, T.; Ogita, N. *J. Comput. Phys.* **1983**, *51*, 191.

(30) Sastry, S.; Corti, D. S.; Debenedetti, P. G.; Stillinger, F. H. *Phys. Rev. E* **1997**, *56*, 5524.